# 4

# Improved Signal-to-Noise in Proton Spectroscopy of the Human calf Muscle at 7 Tesla Using Localized $B_1$ Calibration

*Maarten J. Versluis*
*Hermien E. Kan*
*Mark A. van Buchem*
*Andrew G. Webb*

**Magnetic Resonance in Medicine 2010;63: 207-211**

## ABSTRACT

Large variations of tip angle within a slice can lead to suboptimal pulse power optimization using standard techniques, which measure the average tip angle over a slice: this effect is especially pronounced at fields of 7 T and above. A technique is introduced that performs a volume-selective power optimization in less than 10 seconds, and automatically calibrates the radio-frequency (RF) pulses for subsequent spectroscopy scans. Using this technique, MR spectra were acquired in the human calf of seven healthy volunteers with a partial volume Tx / Rx coil. Increases in signal-to-noise-ratio (SNR) based upon the unsuppressed water signal between 22 ± 5% and 166 ± 42%, compared to spectra obtained with the conventional power calibration technique, were measured in different regions of the calf muscle. This new technique was able to measure the inhomogeneous RF field at 7 T and resulted in a considerable SNR increase.

## INTRODUCTION

Human MRI at high magnetic fields, i.e., 7T and above, has to overcome a large variation in the strength of the radiofrequency field ($B_1$) over the imaging volume. The primary, intrinsic reason is that the wavelength of the corresponding radiofrequency (RF) excitation and reception is less than, or comparable to, the dimensions of the body. The second, more practical reason is that the lack of a body coil, particularly on commercial systems, leads to a more frequent use of local Tx / Rx surface coils than at lower field. Both of these factors result in accurate tip angle calibration techniques being very important for obtaining the optimal SNR. Conventional methods used commonly at lower field strengths, which measure the tip angle averaged over a slice or over the complete sensitive volume of the coil (1, 2) lead to suboptimal results at high field, as outlined by a recent article on 7 T cardiac imaging (3).

Many different approaches have been proposed for $B_1$ mapping, including those based on repeated measurements with different tip angles (4–6), different repetition times (7), measuring the ratio between the signal intensity from spin echoes and stimulated echoes (1, 2, 8, 9), and detecting tip angle related phase changes (10). These methods can be divided in two categories: first, those that use gradients to encode the entire volume and calculate the tip angle on a pixel-by-pixel basis (4–10), and second, those that measure the tip angle over a large volume using non-selective, or slice-selective RF pulses (1, 2). Methods in the first category tend to be lengthy procedures and are therefore not suitable for use as a calibration sequence in a clinical setting. Methods in the second category are fast but lead to inaccurate results when the $B_1$ distribution is very inhomogeneous.

In this work, a simple technique is introduced that measures the tip angle in a small volume of interest (VOI) using four slice-selective RF pulses. The method, which we have called volume-selective power optimization ($PO_{volume}$), measures the ratio of the signal from two stimulated echoes (STE) to calculate the average tip angle in the VOI. The optimal value is found by an iterative approach, and this value is used to automatically calibrate the RF amplifier. Since only a small volume is measured, the technique is very fast (2s per iteration). Experiments such as single voxel spectroscopy are expected to benefit most because of the high sensitivity of the signal intensity to suboptimal power settings of the three RF pulses used for localization.

In this study, we compared the SNR of localized MR spectra in the calf acquired with this new technique with a conventional three pulse calibration

technique ($PO_{slice}$), the standard on most commercial MR systems that averages the measured tip angle over a slice through the center of the VOI (2).

## METHODS

All experiments were performed on a commercial 7 T Philips Achieva MRI scanner (Philips Healthcare, Best, The Netherlands). A quadrature half-volume Tx/Rx coil was constructed for the human calf. Two square loops of dimensions 10 cm were constructed from copper tape (1 cm wide, 25 μm thick), which was fixed to a flexible Teflon former (2 mm thickness). The loops were capacitively split into sections ~5 cm in length, corresponding to $1/20^{th}$ of the RF wavelength at 7 T. The two loops were overlapped by ~10% to minimize mutual inductance. Balanced impedance matching using variable capacitors and a lattice balun were used for each excitation port, which were fed from the quadrature outputs of the Philips transmit/receive interface box. The entire coil assembly was mounted on a rigid semi-cylindrical plexiglass former (thickness 5 mm, inner diameter 15 cm). A layer of foam, ~1 cm thick, was placed inside the cylinder, and the subject's lower leg lay on top of this foam layer.

### *Subjects*

Seven volunteers (6 males, 1 female, age 37 ± 9 years) were scanned and localized spectra were obtained at multiple locations with respect to the coil. In addition, a $B_1$ map was obtained from one volunteer to show the RF homogeneity of the coil. Informed consent was obtained from all subjects in accordance with guidelines of the local medical ethics committee.

### *Calibration sequence*

The power of the RF amplifier was calibrated by measuring the tip angle in a VOI using the ratio of the signal intensities from two stimulated echoes for the four-pulse sequence shown in Figure 1. A three-dimensional volume was selected using four slice-selective RF pulses. The first three pulses were applied with the gradients in orthogonal directions, with the fourth RF pulse applied simultaneously with the gradient in the same direction as during the third RF pulse. The resulting stimulated echo signals were acquired. All other free induction decay and echo pathways were carefully spoiled using crusher gradients.

The ratio of the two STE signals, $I_{STE2}$ and $I_{STE1}$, is given by (11):

$$\frac{I_{STE_2}}{I_{STE_1}} = \frac{\sin\alpha_3 \cos\alpha_2 \exp\left(\frac{-(\tau_2+\tau 3)}{T_1}\right)}{\sin\alpha_2 \exp\left(\frac{-\tau_2}{T_1}\right)} \quad \textbf{[1]}$$

where $\alpha_i$ denotes the RF pulse angle for the different pulses, and $\tau_i$ denotes the time at which each RF pulse is applied. When $\alpha_2$ equals $\alpha_3$ Eq. [1] reduces to:

$$\frac{I_{STE_2}}{I_{STE_1}} = \cos\alpha_2 \exp\left(\frac{-\tau_3}{T_1}\right) \quad \textbf{[2]}$$

The value of $\tau_3$ is chosen such that $\tau_3 << T_1$ (12). Therefore the tip angle can be accurately estimated for the selected volume using the following equation:

$$\alpha_2 \approx \cos^{-1}\left(\frac{I_{STE_2}}{I_{STE_1}}\right) \quad \textbf{[3]}$$

For the pulse sequence in Figure 1, the maximum signal intensity for the $STE_2$ signal occurs when the tip angle for $\alpha_0$ and $\alpha_1$ is 90°, and 45° for $\alpha_2$ and $\alpha_3$.

The volume for the $PO_{volume}$ was identical to the VOI of the spectroscopy experiment that followed the calibration sequence. The following parameters were used: repetition time (TR) / $TE_{STE1}$ / $TE_{STE2}$ = 2000 ms / 31 ms/ 51 ms. The tip angle in the VOI was calculated online and was used for the next iteration to set the RF amplifier. When the measured tip angle deviated more than 3 degrees from the requested tip angle a new iteration was performed with updated settings based on the last iteration: a maximum of 5 iterations was used to reach the desired tip angle. Regions with low signal can lead to an invalid signal ratio ($I_{STE2}$ / $I_{STE2}$ > 1) due to noise influences. These values were not accepted and the sequence was performed again with higher RF amplifier power settings; in this way each region produced results consistent with equation [3].

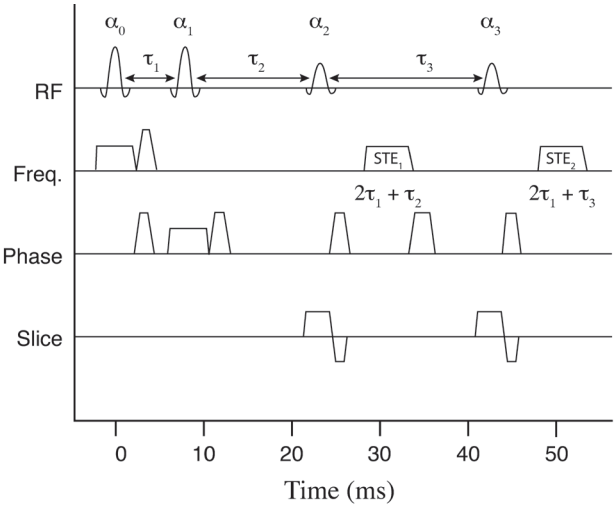


**Figure 1: Sequence diagram of the volume selective RF calibration technique.**
A volume is selected using four RF pulses and gradients. Targeted angles for maximum signal intensity of $STE_2$ are $\alpha_0 = \alpha_1 = 90°$ and $\alpha_2 = \alpha_3 = 45°$. Two stimulated echoes are acquired ($STE_1$ and $STE_2$) at times $2\tau_1+\tau_2$ and $2\tau_1+\tau_3$ respectively, while the spin-echo and free induction decay pathways are spoiled using crusher gradients on all three axes. The intervals between the RF pulses are: $\tau_1 = 8$ ms, $\tau_2 = 15$ ms and $\tau_3 = 19.5$ ms.

The sequence was performed twice, both before and after shimming and determination of the water resonance frequency ($f_0$). Both shimming and $f_0$ determination were performed using adiabatic pulses, which are relatively insensitive to variations in RF power. Image based shimming (13) as provided by the manufacturer was used for regions where conventional shimming failed.

The conventional slice-selective calibration method was measured with the slice oriented along the slice selection direction of the VOI, which was, depending on the exact orientation of the voxel, approximately perpendicular to the coil.

*Localized spectroscopy*

The new calibration technique was evaluated in several stimulated echo acquisition mode (STEAM) MR spectra of the calf muscle. The following scan parameters were used: 10x10x10 $mm^3$ voxel, TR = 2000 ms, mixing time (TM) = 25 ms, echo time (TE) = 25 ms, 64 averages. The total scan duration including optimization of the water suppression was approximately 4 minutes, a clinically acceptable timeframe for patient studies. The coil was placed on the posterior side of the leg and positioned approximately at the location of the largest circumference of the calf. MR spectra were obtained at different

locations in the calf muscles, one set using the standard power calibration sequence over the entire slice, and the other set with the new four-pulse volume-selective calibration technique. In addition, for both scans a non-water suppressed scan with the same settings as the water suppressed scan was acquired to measure SNR using eight averages. The VOIs for the spectroscopy scans were positioned in the central zone of the soleus muscle (SOL), the medial side of the gastrocnemius muscle (GM) and in two different locations in the medial side of the soleus muscle (SM) based on a $T_1$ -weighted anatomical image acquired with the following parameters: TR / TE / flip angle (FA) = 300 ms/ 5.2 ms/ 30°, voxel = 0.5 x 0.5 x 4 $mm^3$, field-of-view (FOV) = 180 x 180 x 66 $mm^3$, 15 slices, scan duration is two minutes.

The spectra were viewed in jMRUI (14) and the AMARES algorithm (15) was used to fit the water peak based on a Lorentzian line shape. The SNR of the spectra was measured by dividing the integrated area under the fitted water peak of the non-water-suppressed scans by the standard deviation of the last 200 points of the time-domain signal, which contained only noise. The water signal was chosen because the intensity is much larger than that of any metabolite and since residual dipolar couplings and bulk susceptibility effects can hamper accurate quantification of metabolite signals in muscle (16).

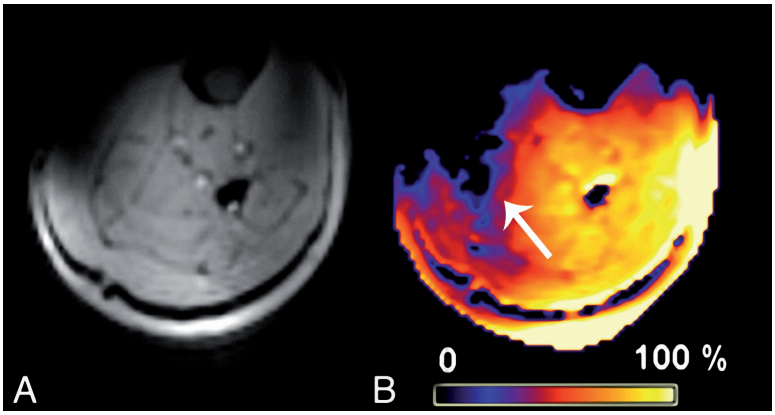


**Figure 2: Coverage and $B_1$-profile of coil.**
The left image (a) shows a single slice from a low resolution 3D gradient echo sequence of the calf muscle. The right image (b) shows the corresponding $B_1$ map scaled as a percentage of the target $B_1$. There is substantial variation of $B_1$ over the leg as would be expected for the partial volume Tx / Rx coil that was used in the experiments. Especially towards the medial side of the leg the $B_1$ inhomogeneity is particularly pronounced as depicted by the arrow.

*$B_1$ mapping*

A $B_1$ map was acquired using a 3D spoiled gradient echo sequence with two interleaved repetition times ($TR_1$ and $TR_2$) with the following parameters: $TR_1$ / $TR_2$ / TE / FA = 20 ms/ 100 ms/ 1.8 ms/ 30°, voxel = 2 x 2 x 4 $mm^3$, FOV = 180 x 180 x 116 $mm^3$, total scan duration is two-and-a –half minutes. The ratio of the resulting images with different TR yields a tip angle distribution map (7).

## RESULTS

Figure 2 shows a single slice from the 3D $B_1$ map illustrating that the tip angle varies considerably over the field-of-view, and that the excitation pattern is not symmetric. The latter observation is in line with several previous studies carried out at high field (17). The sensitive region of the coil is large enough to almost completely cover the soleus and gastrocnemius muscles, and the tip angle varies by more than a factor-of-two over this region. Toward the SM on the medial side of the leg there is a region where the $B_1$ inhomogeneity is particularly pronounced. Differences were found in the result of the calibration sequence before and after $f_0$ determination and shimming when the VOI was moved from the SOL to the SM.

Figure 3a shows the approximate locations of three volumes from which localized spectra were obtained. For all volunteers, the $PO_{volume}$ calibration sequence iteratively arrived at the desired pulse angle for the selected volume. At the location of the SM conventional volume shimming failed due to the high $B_1$ inhomogeneities, therefore image based shimming was used. MR spectra in the SM were acquired at two different locations within the same volunteer because of the high variability in $B_1$ in that region. Increases in SNR were found in all locations when compared to the standard $PO_{slice}$ technique. The amount of SNR increase was dependent on the location with respect to the coil. Representative spectra from the SOL are shown in figure 3b and spectra from the SM are shown in figure 3c. The bottom spectrum is acquired with the $PO_{slice}$ technique, whereas the one at the top is acquired with the $PO_{volume}$ technique. The $PO_{volume}$ technique results in an increase in SNR of 24% and 224% for SOL and SM, respectively, in this volunteer, based upon the unsuppressed water signal.

Figure 4 shows the SNR increases averaged over all volunteers for different regions in the calf muscles. The measured increases in SNR were 34 ± 5% in the GM, 22 ± 5% in the SOL and 166 ± 42% in the SM based upon the unsuppressed water signal.

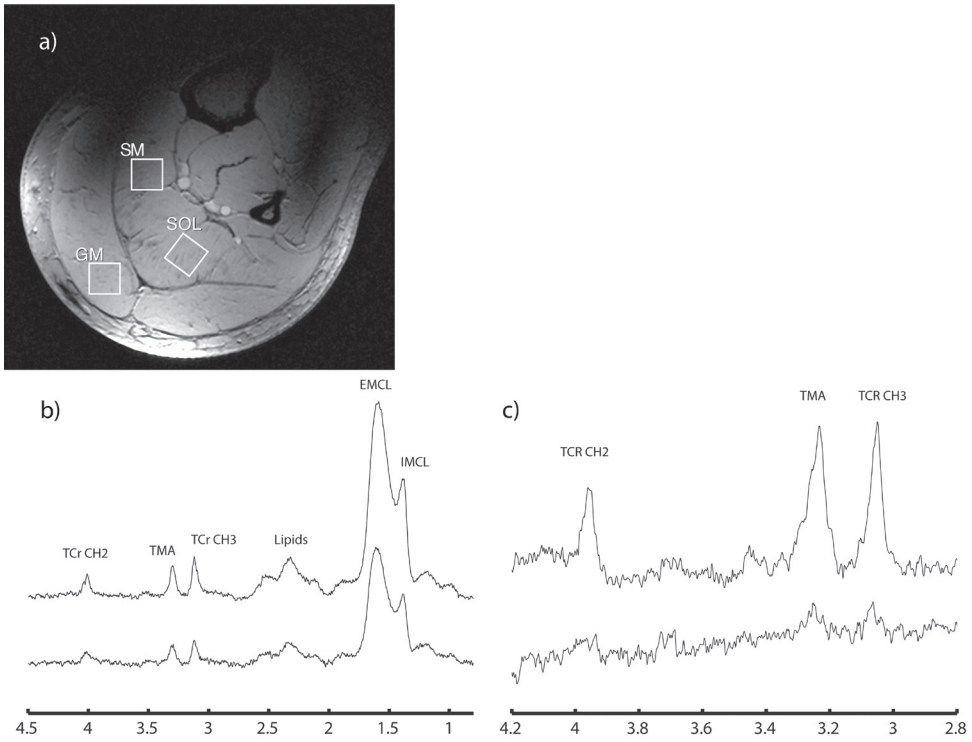


**Figure 3: Anatomic image and acquired MR spectra.**
(a) $T_1$-weighted anatomical image for reference showing the locations where the MR spectra were obtained. (b) Localized MR spectra of the SOL of a volunteer, top: $PO_{volume}$ , bottom: $PO_{slice}$. (c) Localized MR spectra of the SM, top: $PO_{volume}$ , bottom: $PO_{slice}$. Note the clear increase in SNR of the spectra from the new volume-selective power optimization method. Based on the signal intensity of the water peak (not displayed) an SNR increase of 24% was found in (b) and 224% in (c). Scan parameters: STEAM sequence, 10x10x10 $mm^3$ voxel, TR/ TM / TE = 2000 ms/ 25 ms/ 25 ms, 64 averages. Volumes were placed in the central zone of the soleus muscle (SOL), the medial side of the gastrocnemius muscle (GM) and the medial side of the soleus muscle (SM).

## DISCUSSION

Partial volume Tx/Rx coils are consistently used for studies at high field (18), particularly those aimed at very high spatial resolution and/ or reduced specific absorption rate. In addition to the intrinsic non-uniformity of the $B_1$ field from such coils, asymmetries in the transmit field are induced by the interaction of the RF field with the dielectric properties of the tissue. The resulting $B_1$ fields are not easy to predict, and so experimental procedures for optimizing local tip angles are important. Since most MRS studies involve multiple-pulse localized spectroscopy experiments, sub-optimal pulse calibration in the volume of interest can reduce signal intensities significantly.

This is particularly important in clinical studies, where total data acquisition times are typically limited both by institutional review boards and by patient comfort. Using a new four-pulse volume-selective optimization method consistent increases in SNR of the MR spectra were found compared to the standard slice-selective method (1, 2). When the tip angle is averaged over a large area the calibration is strongly biased toward the area with the highest $B_1$, which is not necessarily near the VOI. This is particularly true for partial volume and surface Tx/Rx coils, which have a highly non uniform excitation profile. Using the four-pulse volume-selective optimization method we were able to locally measure the $B_1$ field. In contrast to many other $B_1$ mapping procedures (4–10) only signal originating from the VOI was acquired and therefore the calculations required for iterative convergence to the optimal tip angle are simple and can be performed real-time. The procedure was fast enough (less than 10 s) to be used as a calibration sequence before the actual MRS sequence.

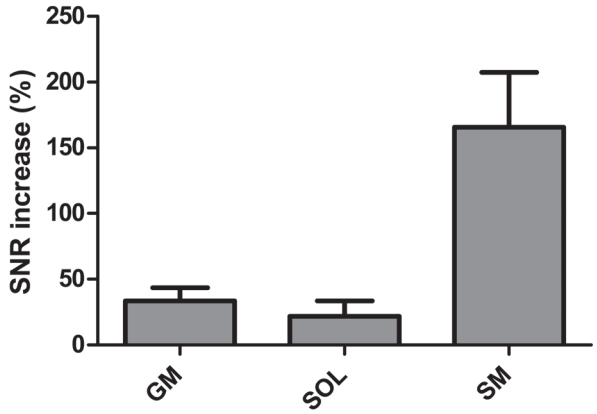


**Figure 4: SNR comparisons of the unsuppressed water spectra.**
Spectra were acquired in different locations in the calf muscle, GM (n = 4), SOL (n = 5) and SM (n = 4) subjects. For the SM two different locations within the same volunteer were measured. A large variation in SNR increase was measured in the SM because of the very high $B_1$ inhomogeneities at that location. The SNR was determined using the area under the water peak of a non-water suppressed spectrum divided by the standard deviation of the last 200 points of the time signal. Error bars represent standard error of the mean.

The technique is valid under the assumption that $T_1$ decay between the two stimulated echoes can be neglected. This is usually valid in vivo where $T_1$ values of tissue are typically two orders of magnitude larger than the time between the first and second stimulated echo signal (12, 19). Therefore, the method is not only limited for use in the calf muscle but could also be used in the human brain. However if the technique is applied in tissues with very

short $T_1$ values such as fat, it may be necessary to correct for the $T_1$ decay during the calibration sequence. Both stimulated echo signals have identical $T_2$ decay, and therefore no errors are introduced for tissues with different $T_2$ values. However tissues with very short $T_2$ values will result in lower SNR and therefore increase the difficulty in obtaining a reliable tip angle estimation. The TE of the calibration sequence was 16 ms which was short enough to reliably measure signal in the human calf muscle.

The first iteration of the volume-selective technique is performed using the $f_0$ and shim settings of the previous scan. Therefore a large change in the location of the VOI can lead to a large change in $f_0$ and shim settings. This was the case when the VOI was moved from the SOL to the SM, and so it was necessary to repeat the $PO_{volume}$ sequence again after shimming and frequency adjustment

The SNR gain for the SOL was measured to be the smallest compared to the other two locations. This part of the muscle is located in a rather homogeneous sensitivity region of the coil and the difference between $PO_{slice}$ and $PO_{volume}$ is therefore small, but nevertheless significant, corresponding to a reduction in scan time of approximately 40% to achieve a given SNR. The GM is located closer to the coil but within a more inhomogeneous region and consequently a larger SNR increase is both expected and measured when comparing the two techniques. The $B_1$ inhomogeneity around the SM is very pronounced and therefore the largest SNR increases are found in this region because the slice-selective power calibration method is not able to accurately measure the local $B_1$ field. The increase in SNR in the SM is therefore also strongly dependent on the exact location of the VOI, but is typically substantial. The reported SNR increases are measured using the unsuppressed water signals for improved accuracy: however, the metabolite SNR should increase proportionally given the similar relaxation properties of the metabolites and water (12). Visual inspection of the spectra in the figures does indeed show this increase.

In summary, increases of up to 166% in SNR based upon the unsuppressed water signal were found in calf spectra of five healthy volunteers. This results in significant reduction in scan time, while maintaining the same SNR, an important factor when obtaining spectra in a clinical setting. Even with “homogeneous” transmit coils, the variation in tip angles is known to be pronounced and patient-specific, and so simple experimentally-based power optimization schemes are valuable in realizing the full signal-to-noise potential of high field.

## REFERENCES


1. Carlson JW, Kramer DM. Rapid radiofrequency calibration in MRI. Magn Reson Med 1990 ;15:438–45.
2. Perman WH, Bernstein MA, Sandstrom JC. A method for correctly setting the rf flip angle. Magn Reson Med 1989 ;9:16–24.
3. Snyder CJ, DelaBarre L, Metzger GJ, Moortele P-F van de, Akgun C, Ugurbil K, Vaughan JT. Initial results of cardiac imaging at 7 tesla. Magnetic Resonance in Medicine 2009 ;61:517–524.
4. Insko EK, Bolinger L. Mapping of the Radiofrequency Field. Journal of Magnetic Resonance, Series A 1993 ;103:82–85.
5. Stollberger R, Wach P. Imaging of the active B1 field in vivo. Magn Reson Med 1996 ;35:246–51.
6. Wang J, Qiu M, Yang QX, Smith MB, Constable RT. Measurement and correction of transmitter and receiver induced nonuniformities in vivo. Magnetic Resonance in Medicine 2005 ;53:408–417.
7. Yarnykh VL. Actual flip-angle imaging in the pulsed steady state: A method for rapid three-dimensional mapping of the transmitted radiofrequency field. Magnetic Resonance in Medicine 2007 ;57:192–200.
8. Counsell CJR. Stimulated Echoes and Spin Echoes. Simultaneous Determination of T2, Diffusion Coefficient, and RF Homogeneity. Journal of Magnetic Resonance, Series B 1993 ;101:28–34.
9. Akoka S, Franconi F, Seguin F, Le Pape A. Radiofrequency map of an NMR coil by imaging. Magnetic Resonance Imaging 1993 ;11:437–441.
10. Oh CH, Hilal SK, Cho ZH, Mun IK. Radio frequency field intensity mapping using a composite spin-echo sequence. Magnetic Resonance Imaging 1990 ;8:21–25.
11. Liang Z-P, Lauterbur PC. Principles of Magnetic Resonance Imaging: A Signal Processing Perspective.
12. Wang L, Nouha Salibi, Yan Wu, Mark E. Schweitzer, Ravinder R. Regatte. Relaxation times of skeletal muscle metabolites at 7T. Journal of Magnetic Resonance Imaging 2009 ;29:1457–1464.
13. Schär M, Kozerke S, Fischer SE, Boesiger P. Cardiac SSFP imaging at 3 Tesla. Magnetic Resonance in Medicine 2004 ;51:799–806.
14. Naressi A, Couturier C, Devos JM, Janssen M, Mangeat C, de Beer R, Graveron-Demilly D. Java-based graphical user interface for the MRUI quantitation package. MAGMA 2001 ;12:141–52.
15. Vanhamme, van den Boogaart A, Van Huffel S. Improved method for accurate and efficient quantification of MRS data with use of prior knowledge. J Magn Reson 1997 ;129:35–43.
16. Boesch C. Musculoskeletal spectroscopy. J Magn Reson Imaging 2007 ;25:321–338.
17. Collins CM, Smith MB. Calculations of B1 distribution, SNR, and SAR for a surface coil adjacent to an anatomically-accurate human body model. Magnetic Resonance in Medicine 2001 ;45:692–699.
18. Ren J, Dimitrov I, Sherry AD, Malloy CR. Composition of adipose tissue and marrow fat in humans by 1H NMR at 7 Tesla. J. Lipid Res. 2008 ;49:2055–2062.

19. Wright P, Mougin O, Totman J, Peters A, Brookes M, Coxon R, Morris P, Clemence M, Francis S, Bowtell R, Gowland P. Water proton T 1 measurements in brain tissue at 7, 3, and 1.5T using IR-EPI, IR-TSE, and MPRAGE: results and optimization. Magnetic Resonance Materials in Physics, Biology and Medicine 2008 ;21:121–130.